

ASXL1 Mutations Promote Myeloid Transformation through Loss of PRC2-Mediated Gene Repression

Omar Abdel-Wahab,^{1,12} Mazhar Adli,^{2,12} Lindsay M. LaFave,^{1,3,12} Jie Gao,⁵ Todd Hricik,¹ Alan H. Shih,¹ Suveg Pandey,¹ Jay P. Patel,¹ Young Rock Chung,¹ Richard Koche,² Fabiana Perna,⁴ Xinyang Zhao,⁶ Jordan E. Taylor,⁷ Christopher Y. Park,¹ Martin Carroll,⁸ Ari Melnick,⁹ Stephen D. Nimer,¹¹ Jacob D. Jaffe,⁷ Iannis Aifantis,⁴ Bradley E. Bernstein,^{2,*} and Ross L. Levine^{1,10,*}

¹Human Oncology and Pathogenesis Program and Leukemia Service, Memorial Sloan-Kettering Cancer Center, 1275 York Avenue, Box 20, New York, NY 10065, USA

²Howard Hughes Medical Institute, Broad Institute of Harvard and MIT, Department of Pathology, Massachusetts General Hospital, and Harvard Medical School, MGH-Simches Research Building, CPZN 8400, 185 Cambridge Street, Boston, MA 02114, USA

³Gerstner Sloan Kettering School of Biomedical Sciences

⁴Molecular Pharmacology and Chemistry Program
Memorial Sloan-Kettering Cancer Center, New York, NY 10065, USA

⁵Howard Hughes Medical Institute and Department of Pathology, New York University School of Medicine, New York, NY 10016, USA

⁶Department of Biochemistry and Molecular Genetics, University of Alabama, Birmingham, AL 35233, USA

⁷Broad Institute of Harvard and MIT, Cambridge, MA 02142, USA

⁸Division of Hematology and Oncology, University of Pennsylvania, Philadelphia, PA 19104, USA

⁹Division of Hematology/Oncology

¹⁰Biochemistry and Molecular Biology Program
Weill Cornell Medical College, New York, NY 10065, USA

¹¹Sylvester Comprehensive Cancer Center, University of Miami, Miami, FL 33136, USA

¹²These authors contributed equally to this work

*Correspondence: bernstein.bradley@mgh.harvard.edu (B.E.B.), leviner@mskcc.org (R.L.L.)
<http://dx.doi.org/10.1016/j.ccr.2012.06.032>

SUMMARY

Recurrent somatic *ASXL1* mutations occur in patients with myelodysplastic syndrome, myeloproliferative neoplasms, and acute myeloid leukemia, and are associated with adverse outcome. Despite the genetic and clinical data implicating *ASXL1* mutations in myeloid malignancies, the mechanisms of transformation by *ASXL1* mutations are not understood. Here, we identify that *ASXL1* mutations result in loss of polycomb repressive complex 2 (PRC2)-mediated histone H3 lysine 27 (H3K27) tri-methylation. Through integration of microarray data with genome-wide histone modification ChIP-Seq data, we identify targets of *ASXL1* repression, including the posterior *HOXA* cluster that is known to contribute to myeloid transformation. We demonstrate that *ASXL1* associates with the PRC2, and that loss of *ASXL1* in vivo collaborates with *NRASG12D* to promote myeloid leukemogenesis.

INTRODUCTION

Recent genome-wide and candidate-gene discovery efforts have identified a series of novel somatic genetic alterations in patients with myeloid malignancies with relevance to pathogen-

esis, prognostication, and/or therapy. Notably, these include mutations in genes with known or putative roles in the epigenetic regulation of gene transcription. One such example is the mutations in the gene *Addition of sex combs-like 1* (*ASXL1*), which is mutated in $\approx 15\%$ – 25% of patients with myelodysplastic

Significance

Mutations in genes involved in modification of chromatin have recently been identified in patients with leukemias and other malignancies. Here, we demonstrate a specific role for *ASXL1*, a putative epigenetic modifier frequently mutated in myeloid malignancies, in polycomb repressive complex 2 (PRC2)-mediated transcriptional repression in hematopoietic cells. *ASXL1* loss-of-function mutations in myeloid malignancies result in loss of PRC2-mediated gene repression of known leukemogenic target genes. Our data provide insight into how *ASXL1* mutations contribute to myeloid transformation through dysregulation of Polycomb-mediated gene silencing. This approach also demonstrates how epigenomic and functional studies can be used to elucidate the function of mutations in epigenetic modifiers in malignant transformation.

syndrome and $\approx 10\%$ – 15% of patients with myeloproliferative neoplasms and acute myeloid leukemia (Abdel-Wahab et al., 2011; Bejar et al., 2011; Gelsi-Boyer et al., 2009). Clinical studies have consistently indicated that mutations in *ASXL1* are associated with adverse survival in myelodysplastic syndrome and acute myeloid leukemia (Bejar et al., 2011; Metzeler et al., 2011; Pratorcorona et al., 2012; Thol et al., 2011).

ASXL1 is the human homolog of *Drosophila Additional sex combs (Asx)*. *Asx* deletion results in a homeotic phenotype characteristic of both Polycomb (PcG) and Trithorax group (TxG) gene deletions (Gaebler et al., 1999), which led to the hypothesis that *Asx* has dual functions in silencing and activation of homeotic gene expression. In addition, functional studies in *Drosophila* suggested that *Asx* encodes a chromatin-associated protein with similarities to PcG proteins (Sinclair et al., 1998). More recently, it was demonstrated that *Drosophila Asx* forms a complex with the chromatin deubiquitinase Calypso to form the Polycomb-repressive deubiquitinase (PR-DUB) complex, which removes monoubiquitin from histone H2A at lysine 119. The mammalian homolog of Calypso, BAP1, directly associates with ASXL1, and the mammalian BAP1-ASXL1 complex was shown to possess deubiquitinase activity in vitro (Scheuermann et al., 2010).

The mechanisms by which *ASXL1* mutations contribute to myeloid transformation have not been delineated. A series of in vitro studies in non-hematopoietic cells have suggested a variety of activities for ASXL1, including physical cooperativity with HP1a and LSD1 to repress retinoic acid-receptor activity and interaction with peroxisome proliferator-activated receptor gamma (PPAR γ) to suppress lipogenesis (Cho et al., 2006; Lee et al., 2010; Park et al., 2011). In addition, a recent study using a gene-trap model reported that constitutive disruption of *Asx1* results in significant perinatal lethality; however, the authors did not note alterations in stem/progenitor numbers in surviving *Asx1* gene trap mice (Fisher et al., 2010a, 2010b). Importantly, the majority of mutations in *ASXL1* occur as nonsense mutations and insertions/deletions proximal or within the last exon prior to the highly conserved plant homeo domain. It is currently unknown whether mutations in *ASXL1* might confer a gain-of-function due to expression of a truncated protein, or whether somatic loss of ASXL1 in hematopoietic cells leads to specific changes in epigenetic state, gene expression, or hematopoietic functional output. The goals of this study were to determine the effects of *ASXL1* mutations on ASXL1 expression as well as the transcriptional and biological effects of perturbations in ASXL1 which might contribute toward myeloid transformation.

RESULTS

ASXL1 Mutations Result in Loss of ASXL1 Expression

ASXL1 mutations in patients with myeloproliferative neoplasms, myelodysplastic syndrome, and acute myeloid leukemia most commonly occur as somatic nonsense mutations and insertion/deletion mutations in a clustered region adjacent to the highly conserved PHD domain (Abdel-Wahab et al., 2011; Gelsi-Boyer et al., 2009). To assess whether these mutations result in loss of ASXL1 protein expression or in expression of a truncated isoform, we performed western blots using N- and C-terminal anti-ASXL1 antibodies in a panel of human myeloid

leukemia cell lines and primary acute myeloid leukemia samples, which are wild-type or mutant for *ASXL1*. We found that myeloid leukemia cells with homozygous frameshift/nonsense mutations in *ASXL1* (NOMO1 and KBM5) have no detectable ASXL1 protein expression (Figure 1A). Similarly, leukemia cells with heterozygous *ASXL1* mutations have reduced or absent ASXL1 protein expression. Western blot analysis of ASXL1 using an N-terminal anti-ASXL1 antibody in primary acute myeloid leukemia samples wild-type and mutant for *ASXL1* revealed reduced/absent full-length ASXL1 expression in samples with *ASXL1* mutations compared to *ASXL1* wild-type samples (Figure S1A available online). Importantly, we did not identify truncated ASXL1 protein products in mutant samples using N- or C-terminal directed antibodies in primary acute myeloid leukemia samples or leukemia cell lines. Moreover, expression of wild-type ASXL1 cDNA or cDNA constructs bearing leukemia-associated mutant forms of ASXL1 revealed reduced stability of mutant forms of ASXL1 relative to wild-type ASXL1, with more rapid degradation of mutant ASXL1 isoforms following cycloheximide exposure (Figure S1B). These data are consistent with ASXL1 functioning as a tumor suppressor with loss of ASXL1 protein expression in leukemia cells with mutant *ASXL1* alleles.

ASXL1 Knockdown in Hematopoietic Cells Results in Upregulated HOXA Gene Expression

Given that *ASXL1* mutations result in loss of ASXL1 expression, we investigated the effects of ASXL1 knockdown in primary hematopoietic cells. We used a pool of small interfering RNAs (siRNA) to perform knockdown of ASXL1 in primary human CD34+ cells isolated from umbilical cord blood. ASXL1 knockdown was performed in triplicate and confirmed by qRT-PCR analysis (Figure 1B), followed by gene-expression microarray analysis. Gene-set enrichment analysis (GSEA) of this microarray data revealed a significant enrichment of genes found in a previously described gene expression signature of leukemic cells from bone marrow of *MLL-AF9* knock-in mice (Kumar et al., 2009), as well as highly significant enrichment of a gene signature found in primary human cord blood CD34+ cells expressing *NUP98-HOXA9* (Figure S1C and Table S1) (Takeda et al., 2006). Specifically, we found that ASXL1 knockdown in human primary CD34+ cells resulted in increased expression of 145 genes out of the 279 genes, which are overexpressed in the *MLL-AF9* gene expression signature ($p < 0.05$, FDR < 0.05). These gene expression signatures are characterized by increased expression of posterior *HOXA* cluster genes, including *HOXA5-9*.

In order to ascertain whether loss of ASXL1 was associated with similar transcriptional effects in leukemia cells, we performed short hairpin RNA (shRNA)-mediated stable knockdown of *ASXL1* in the *ASXL1*-wild-type human leukemia cell lines UKE1 (Figures 1C and 1D) and SET2 (Figure 1D) followed by microarray and qRT-PCR analysis. Gene expression analysis in UKE-1 cells expressing ASXL1 shRNA compared to control cells revealed significant enrichment of the same *HOXA* gene expression signatures as were seen with ASXL1 knockdown in CD34+ cells (Figure 1C and Table S2). Upregulation of 5' *HOXA* genes was confirmed by qRT-PCR in UKE1 (Figure 1D) cells and by western blot analysis (Figure 1D) in SET2 cells expressing ASXL1 shRNA compared to control. Quantitative mRNA profiling (Nanostring nCounter) of the entire *HOXA* cluster revealed

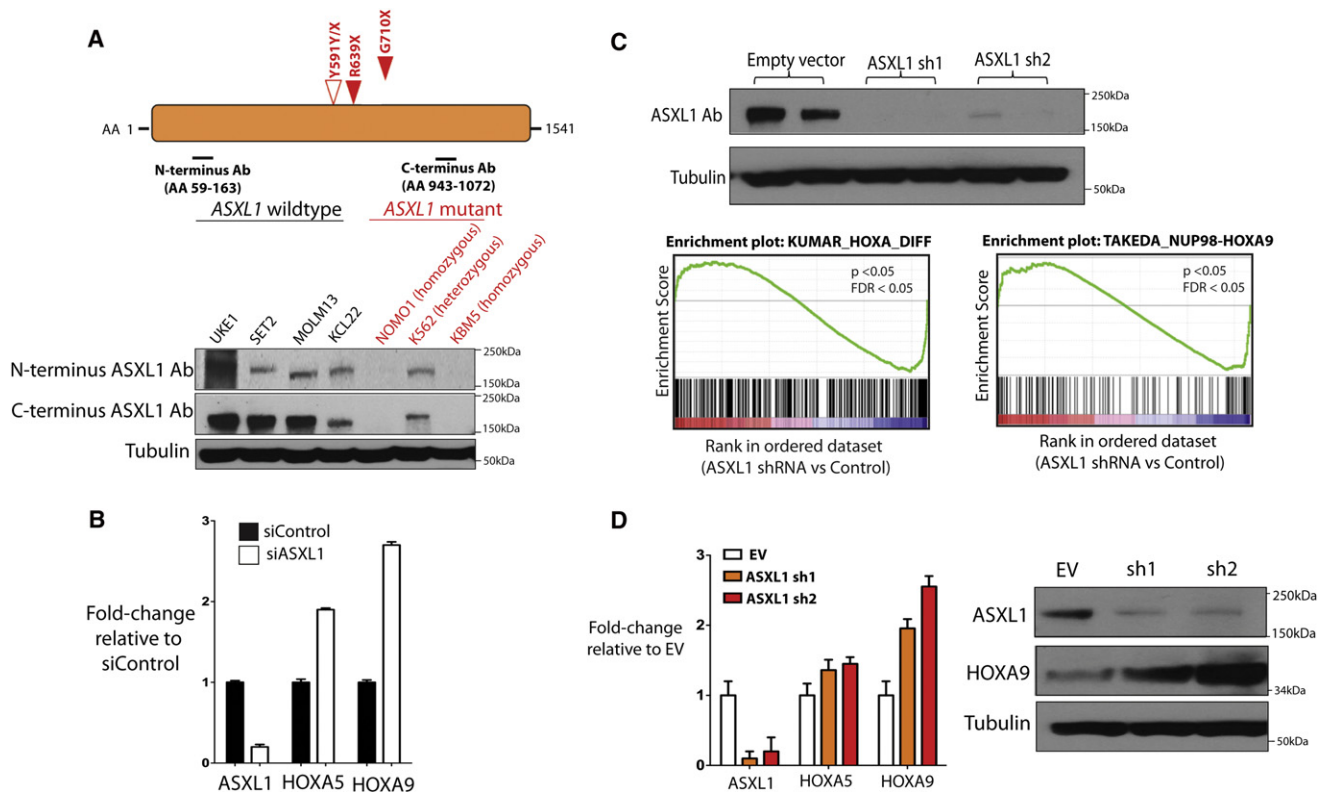


Figure 1. Leukemogenic ASXL1 Mutations Are Loss-of-Function Mutations and ASXL1 Loss Is Associated with Upregulation of HOXA Gene Expression

(A) Characterization of ASXL1 expression in leukemia cells with nonsense mutations in ASXL1 reveals loss of ASXL1 expression at the protein level in cells with homozygous ASXL1 mutations as shown by western blotting using N- and C-terminal anti-ASXL1 antibodies.

(B) Displayed are the ASXL1-mutant cell line lines NOMO1 (homozygous ASXL1 R639X), K562 (heterozygous ASXL1 Y591Y/X), and KBM5 (homozygous ASXL1 G710X) and a panel of ASXL1-wild-type cell lines. ASXL1 siRNA in human primary CD34+ cells from cord blood results in upregulation of HOXA5 and HOXA9 with ASXL1 knockdown (KD) as revealed by quantitative real-time PCR (qRT-PCR) analysis.

(C and D) Stable KD of ASXL1 in ASXL1-wild-type transformed human myeloid leukemia UKE1 cells (as shown by western blot) followed by GSEA reveals significant enrichment of gene sets characterized by upregulation of 5' HOXA genes (C) as was confirmed by qRT-PCR (D). Statistical significance is indicated in (D) by the p value and false-discovery rate (FDR). Similar upregulation of HOXA9 is seen by the western blot following stable ASXL1 KD in the ASXL1-wild-type human leukemia SET2 cells.

Error bars represent standard deviation of expression relative to control. See also Figure S1 and Tables S1 and S2.

upregulation of multiple HOXA members, including HOXA5, 7, 9, and 10, in SET2 cells with ASXL1 knockdown compared to control cells (Figure S1D). These results indicate consistent upregulation of HOXA gene expression following ASXL1 loss in multiple hematopoietic contexts.

ASXL1 Forms a Complex with BAP1 in Leukemia Cells, but BAP1 Loss Does Not Upregulate HoxA Gene Expression in Hematopoietic Cells

Mammalian ASXL1 forms a protein complex in vitro with the chromatin deubiquitinase BAP1, which removes monoubiquitin from histone H2A at lysine 119 (H2AK119) (Scheuermann et al., 2010). In Drosophila loss of either Asx or Calypso resulted in similar effects on genome-wide H2AK119 ubiquitin levels and on target gene expression. Recent studies have revealed recurrent germline and somatic loss-of-function BAP1 mutations in mesothelioma and uveal melanoma (Bott et al., 2011; Harbour et al., 2010; Testa et al., 2011). However, we have not identified BAP1 mutations in patients with myeloproliferative neoplasms or

acute myeloid leukemia (O.A.-W., J.P.P., and R.L.L., unpublished data). Co-immunoprecipitation studies revealed an association between ASXL1 and BAP1 in human myeloid leukemia cells wild-type for ASXL1 but not in those cells mutant for ASXL1 due to reduced/absent ASXL1 expression (Figure 2A). Immunoprecipitation of FLAG-tagged wild-type ASXL1 and FLAG-tagged leukemia-associated mutant forms of ASXL1 revealed reduced interaction between mutant forms of ASXL1 and endogenous BAP1 (Figure S2A). Despite these findings, BAP1 knockdown did not result in upregulation of HOXA5 and HOXA9 in UKE1 cells, although a similar extent of ASXL1 knockdown in the same cells reproducibly increased HOXA5 and HOXA9 expression (Figure 2B). We obtained similar results with knockdown of Asxl1 or Bap1 in the Ba/F3 murine hematopoietic cell line (Figure 2C). In Ba/F3 cells, knockdown of Asxl1 resulted in upregulated Hoxa9 gene expression commensurate with the level of Asxl1 downregulation, whereas knockdown of Bap1 does not impact Hoxa expression (Figure 2C). ASXL1 knockdown in SET-2 cells failed to reveal an effect of ASXL1

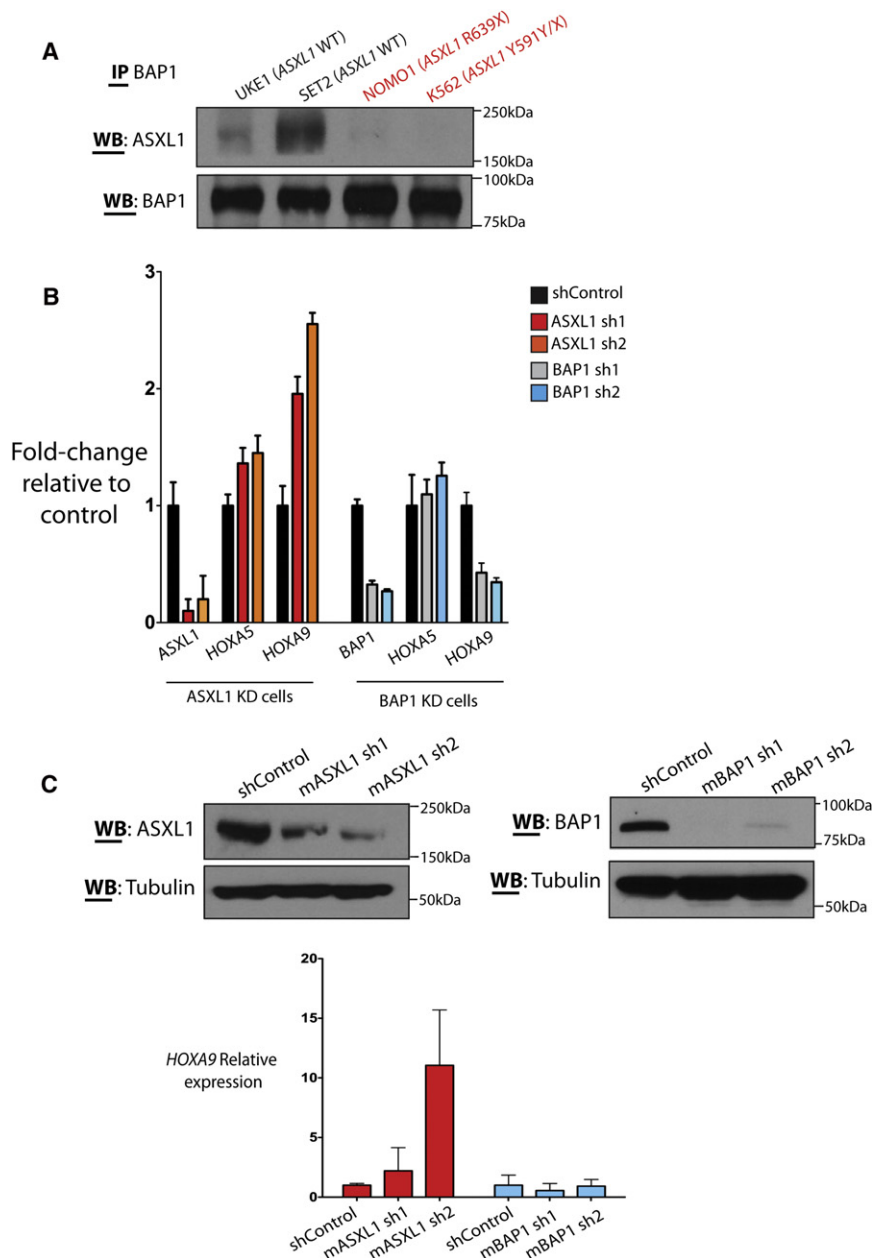


Figure 2. ASXL1 and BAP1 Physically Interact in Human Hematopoietic Cells but BAP1 Loss Does Not Result in Increased *HoxA* Gene Expression

(A) Immunoprecipitation of BAP1 in a panel of ASXL1-wild-type and mutant human myeloid leukemia cells reveals co-association of ASXL1 and BAP1.

(B) Cells with heterozygous or homozygous mutations in ASXL1 with reduced or absent ASXL1 expression have minimal interaction with BAP1 in vitro. BAP1 knockdown in the ASXL1/BAP1 wild-type human leukemia cell line UKE1 fails to alter *HOXA* gene expression. In contrast, stable knockdown of ASXL1 in the same cell type results in a significant upregulation of *HOXA9*.

(C) Similar results are seen with knockdown of *Asx1* or *Bap1* in murine precursor-B lymphoid Ba/F3 cells.

Error bars represent standard deviation of expression relative to control. See also Figure S2.

loss on H2AK119Ub levels as assessed by western blot of purified histones from shRNA control and ASXL1 knockdown cells (Figure S2B). By contrast, SET2 cells treated with MG132 (25 μ M) had a marked decrease in H2AK119Ub, as has been previously described (Dantuma et al., 2006). These data suggest that ASXL1 loss contributes to myeloid transformation through a BAP1-independent mechanism.

Loss of ASXL1 Is Associated with Global Loss of H3K27me3

The results described above led us to hypothesize that ASXL1 loss leads to BAP1-independent effects on chromatin state and on target gene expression. To assess the genome-wide effects of ASXL1 loss on chromatin state, we performed chro-

matin immunoprecipitation followed by next generation sequencing (ChIP-seq) for histone modifications known to be associated with PcG [histone H3 lysine 27 trimethylation (H3K27me3)] or TxG activity [histone H3 lysine 4 trimethylation (H3K4me3)] in UKE1 cells expressing empty vector or two independent validated shRNAs for ASXL1. ChIP-Seq data analysis revealed a significant reduction in genome-wide H3K27me3 transcriptional start site occupancy with ASXL1 knockdown compared to empty vector ($p = 2.2 \times 10^{-16}$; Figure 3A). Approximately 20% of genes ($n = 4,686$) were initially marked by H3K27me3 in their promoter regions (defined as 1.5 kb downstream and 0.5 kb upstream of the transcriptional start site). Among these genes, ~27% had a 2-fold reduction in H3K27me3 ($n = 1,309$) and ~66% had a 1.5-fold reduction in H3K27me3 ($n = 3,092$), respectively, upon ASXL1 knockdown. No significant

effect was seen on H3K4me3 transcriptional start site occupancy with ASXL1 depletion (Figure 3A). We next evaluated whether loss of ASXL1 might be associated with loss of H3K27me3 globally by performing western blot analysis on purified histones from UKE1 cells transduced with empty vector or shRNAs for ASXL1 knockdown. This analysis revealed a significant decrease in global H3K27me3 with ASXL1 loss (Figure 3B), despite preserved expression of the core polycomb repressive complex 2 (PRC2) members EZH2, SUZ12, and EED. Similar effects on total H3K27me3 levels were seen following *Asx1* knockdown in Ba/F3 cells (Figure S3A). These results demonstrate that ASXL1 depletion leads to a marked reduction in genome-wide H3K27me3 in hematopoietic cells.

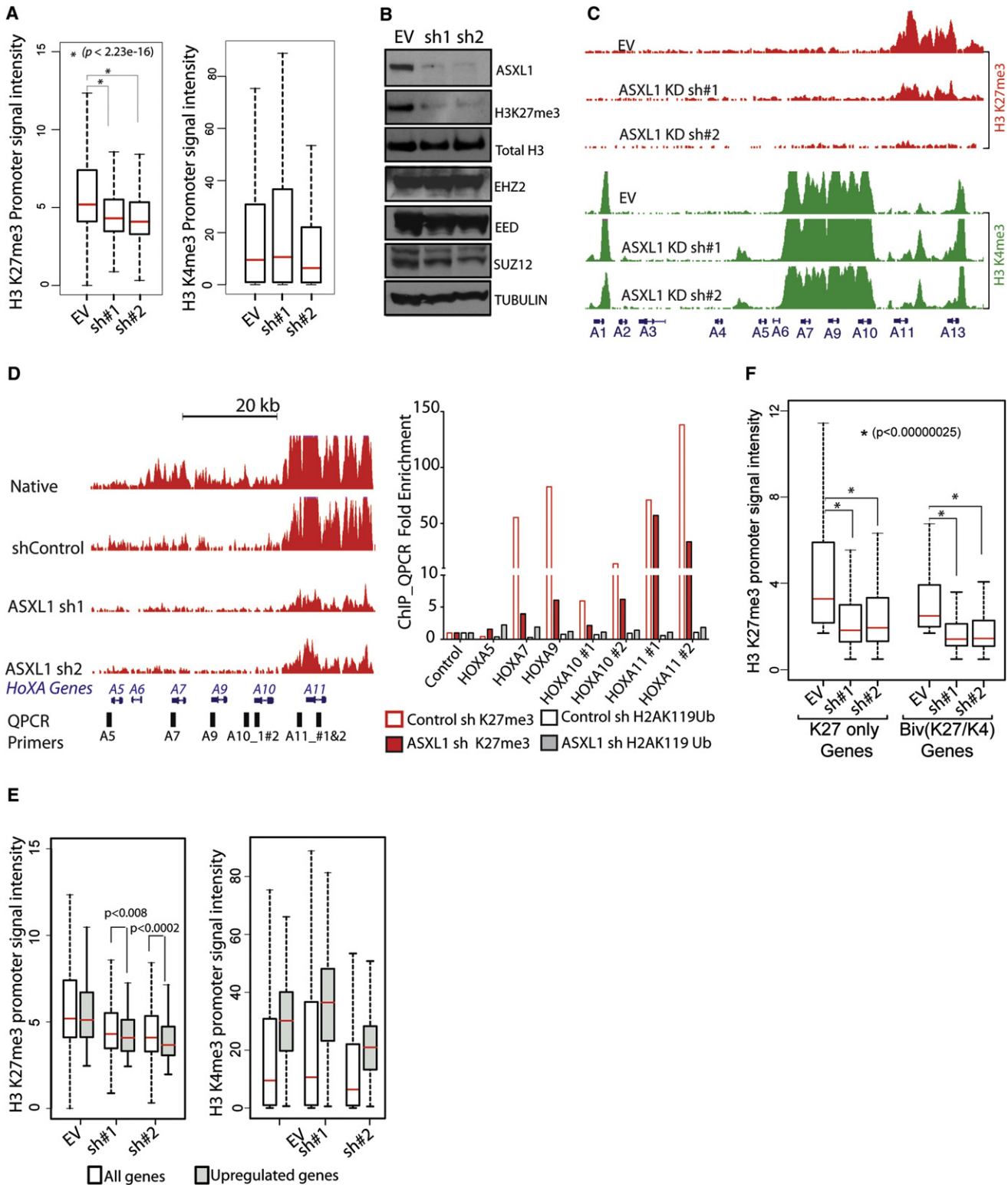


Figure 3. ASXL1 Loss Is Associated with Loss of H3K27me3 and with Increased Expression of Genes Poised for Transcription

(A) ASXL1 loss is associated with a significant genome-wide decrease in H3K27me3 as illustrated by box plot showing the 25th, 50th, and 75th percentiles for H3K27me3 and H3K4me3 enrichment at transcription start sites in UKE1 cells treated with an empty vector or shRNAs directed against ASXL1. The whiskers indicate the most extreme data point less than 1.5 interquartile range from box and the red bar represents the median.

(B) Loss of ASXL1 is associated with a global loss of H3K27me3 without affecting PRC2 component expression as shown by western blot of purified histones from cells with UKE1 knockdown and western blot for core PRC2 component in whole cell lysates from ASXL1 knockdown UKE1 cells.

Detailed analysis of ChIP-seq data revealed that genomic regions marked by large H3K27me3 domains in control cells displayed more profound loss of H3K27me3 upon loss of ASXL1. Genome-wide analysis of the ChIP-Seq data from control and ASXL1 shRNA treated cells revealed that the sites that lose H3K27me3 in the ASXL1 knockdown cells were on average ~6.6 kb in length, while the sites that maintained H3K27me3 were on average ~3.1 kb in length ($p < 10^{-16}$) (Figure S3B). This is visually illustrated by the reduction in H3K27me3 at the posterior *HOXA* cluster (Figure 3C) and at the *HOXB* and *HOXC* loci (Figure S3C). The association of ASXL1 loss with loss of H3K27me3 abundance at the *HOXA* locus was confirmed by ChIP for H3K27me3 in control and ASXL1 knockdown cells followed by qPCR (ChIP-qPCR) across the *HOXA* locus (Figure 3D). ChIP-qPCR in control and knockdown cells revealed a modest increase in H2AK119Ub with ASXL1 loss at the *HOXA* locus (Figure 3D), in contrast to the more significant reduction in H3K27me3. In contrast to the large decrease in H3K27me3 levels at the *HOXA* locus with ASXL1 knockdown, a subset of loci had much less significant reduction in H3K27me3, in particular at loci whose promoters were marked by sharp peaks of H3K27me3 (Figure S3D). Intersection of gene expression and ChIP-Seq data revealed that genes overexpressed in ASXL1 knockdown cells were simultaneously marked with both activating (H3K4me3) and repressive (H3K27me3) domains in control cells (Figures 3E and 3F). This finding suggests that the transcriptional repression mediated by ASXL1 in myeloid cells is most apparent at loci poised for transcription with bivalent chromatin domains. Indeed, the effects of ASXL1 loss on H3K27me3 occupancy were most apparent at genes whose promoters were marked by the dual presence of H3K27me3 and H3K4me3 (Figure 3F). We cannot exclude the possibility that H3K4me3 and H3K27me3 exist in different populations within the homogeneous cell lines being studied, but the chromatin and gene expression data are consistent with an effect of ASXL1 loss on loci with bivalent chromatin domains (Bernstein et al., 2006; Mikkelsen et al., 2007).

Enforced Expression of ASXL1 in Leukemic Cells Results in Suppression of *HOXA* Gene Expression, a Global Increase in H3K27me3, and Growth Suppression

We next investigated whether reintroduction of wild-type ASXL1 protein could restore H3K27me3 levels in ASXL1 mutant leukemia cells. We stably expressed wild-type ASXL1 in NOMO1 and KBM5 cells, homozygous ASXL1 mutant human

leukemia cell lines, which do not express ASXL1 protein (Figure 4A and Figure S4A). ASXL1 expression resulted in a global increase in H3K27me3 as assessed by histone western blot analysis (Figure 4A). Liquid chromatography/mass spectrometry of purified histones in NOMO1 cells expressing ASXL1 confirmed a ~2.5-fold increase in trimethylated H3K27 peptide and significant increases in dimethylated H3K27 in NOMO1 cells expressing ASXL1 compared to empty vector control (Figure 4B). ASXL1 add-back resulted in growth suppression (Figure 4C) and in decreased *HOXA* gene expression in NOMO1 cells (Figure 4D). ASXL1 add-back similarly resulted in decreased expression of *HOXA* target genes in KBM5 cells (Figures S4A and S4B). ChIP-qPCR revealed a strong enrichment in ASXL1 binding at the *HOXA* locus in NOMO1 cells expressing ASXL1, demonstrating that the *HOXA* locus is a direct target of ASXL1 in hematopoietic cells (Figure 4E).

ASXL1 Loss Leads to Exclusion of H3K27me3 and EZH2 from the *HoxA* Cluster Consistent with a Direct Effect of ASXL1 on PRC2 Recruitment

We next investigated whether the effects of ASXL1 loss on H3K27me3 was due to inhibition of PRC2 recruitment to specific target loci. ChIP-qPCR for H3K27me3 in SET2 cells with ASXL1 knockdown or control revealed a loss of H3K27me3 enrichment at the posterior *HoxA* locus with ASXL1 knockdown (Figures 5A and 5B). We observed a modest, variable increase in H3K4me3 enrichment at the *HOXA* locus with ASXL1 depletion in SET2 cells (Figure 5C). We similarly assessed H3K27me3 enrichment in primary bone marrow leukemic cells from acute myeloid leukemia patients, wild-type and mutant for ASXL1, which likewise revealed decreased H3K27me3 enrichment across the *HOXA* cluster in primary acute myeloid leukemia samples with ASXL1 mutations compared to ASXL1-wild-type acute myeloid leukemia samples (Figure 5D).

Given the consistent effects of ASXL1 depletion on H3K27me3 abundance at the *HOXA* locus, we then evaluated the occupancy of EZH2, a core PRC2 member, at the *HoxA* locus. ChIP-Seq for H3K27me3 in native SET2 and UKE1 cells identified that H3K27me3 is present with a dome-like enrichment pattern at the 5' end of the posterior *HOXA* cluster (Figure 5A); ChIP-qPCR revealed that EZH2 is prominently enriched in this same region in parental SET2 cells (Figure 5E). Importantly, ASXL1 depletion resulted in loss of EZH2 enrichment at the *HOXA* locus (Figure 5E), suggesting that ASXL1 is required for EZH2 occupancy and for PRC2-mediated repression of the posterior *HOXA* locus.

(C) Loss of H3K27me3 is evident at the *HOXA* locus as shown by ChIP-Seq promoter track signals across the *HOXA* locus in UKE1 cells treated with an EV or shRNA knockdown of ASXL1.

(D) H3K27me3 ChIP-Seq promoter track signals from *HOXA5* to *HOXA13* in UKE1 cells treated with shRNA control or one of 2 anti-ASXL1 shRNAs with location of primers used in ChIP-quantitative PCR (ChIP-qPCR) validation. ChIP for H3K27me3 and H2AK119Ub followed by ChIP-qPCR in cells treated with control or ASXL1 knockdown confirms a significant decrease in H3K27me3 at the *HOXA* locus with ASXL1 knockdown but minimal effects of ASXL1 knockdown on H2AK119Ub levels at the same primer locations.

(E) Integrating gene-expression data with H3K27me3/H3K4me3 ChIP-Seq identifies a significant correlation between alterations in chromatin state and increases in gene expression following ASXL1 loss at loci normally marked by the simultaneous presence of H3K27me3 and H3K4me3 in control cells.

(F) Loss of H3K27me3 is seen at promoters normally marked by the presence of H3K27me3 alone or at promoters co-occupied by H3K27me3 and H3K4me3 in the control state.

See also Figure S3.

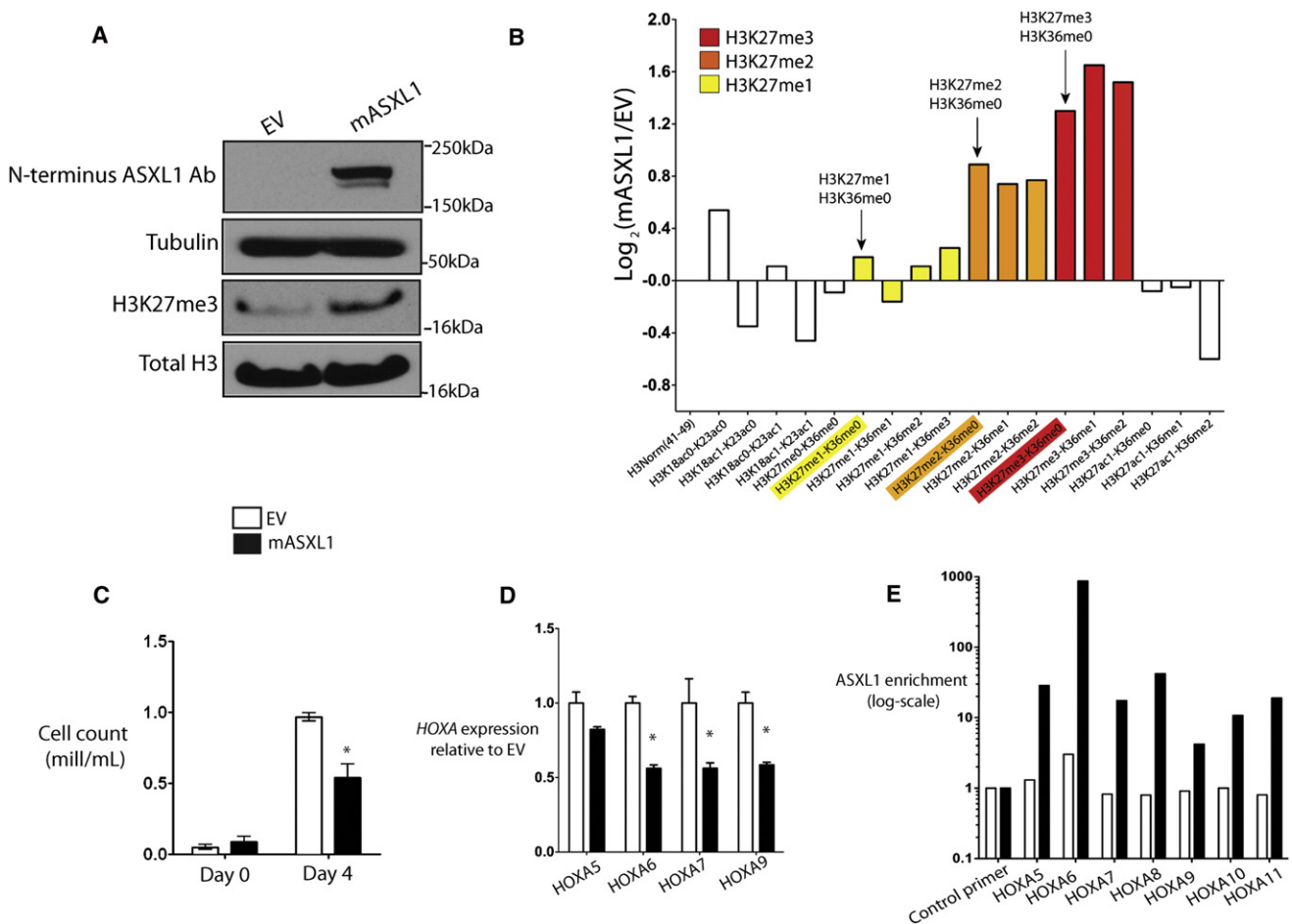


Figure 4. Expression of ASXL1 in ASXL1-Null Leukemic Cells Results in Global Increase in H3K27me2/3, Growth Suppression, and Suppression of *HoxA* Gene Expression

(A and B) ASXL1 expression in ASXL1 null NOMO1 cells is associated with a global increase in H3K27me3 as detected by western blot of purified histones (A) as well as by quantitative liquid-chromatography/mass spectrometry of H3 peptides from amino acids 18–40 (B) (arrows indicate quantification of H3K27me1/2/3). (C) ASXL1 overexpression results in growth suppression in 7-day growth assay performed in triplicate.

(D) Overexpression of ASXL1 was associated with a decrement in posterior *HoxA* gene expression in NOMO1 cells as shown by qRT-PCR for *HOXA5*, 6, 7, and 9. (E) This downregulation in *HOXA* gene expression was concomitant with a strong enrichment of ASXL1 at the loci of these genes as shown by chromatin immunoprecipitation of ASXL1 followed by quantitative PCR with *BCRRP1* as a control locus.

Error bars represent standard deviation of target gene expression relative to control. See also Figure S4.

ASXL1 Physically Interacts with Members of the PRC2 in Human Myeloid Leukemic Cells

Given that ASXL1 localizes to PRC2 target loci and ASXL1 depletion leads to loss of PRC2 occupancy and H3K27me2, we investigated whether ASXL1 might physically interact with the PRC2 complex in hematopoietic cells. Co-immunoprecipitation studies using an anti-FLAG antibody in HEK293T cells expressing empty vector, hASXL1-FLAG alone, or hASXL1-FLAG plus hEZH2 cDNA revealed a clear co-immunoprecipitation of FLAG-ASXL1 with endogenous EZH2 and with ectopically expressed EZH2 (Figure 6A). Similarly, co-immunoprecipitation of FLAG-ASXL1 revealed physical association between ASXL1 and endogenous SUZ12 in 293T cells (Figure 6A). Immunoprecipitations were performed in the presence of benzonase to ensure that the protein-protein interactions observed were DNA-independent (Figure 6B) (Muntean et al., 2010). We then assessed whether endogenous ASXL1 formed a complex with

PRC2 members in hematopoietic cells. We performed IP for EZH2 or ASXL1 followed by western blotting for partner proteins in SET2 and UKE1 cells, which are wild-type for *ASXL1*, *SUZ12*, *EZH2*, and *EED*. These co-immunoprecipitation assays all revealed a physical association between ASXL1 and EZH2 in SET2 (Figure 6B) and UKE1 cells (Figure S5). By contrast, immunoprecipitation of endogenous ASXL1 did not reveal evidence of protein-protein interactions between ASXL1 and BMI1 (Figure S5). Likewise, immunoprecipitation of BMI1 enriched for PRC1 member RING1A, but failed to enrich for ASXL1, suggesting a lack of interaction between ASXL1 and the PRC1 repressive complex (Figure 6C).

ASXL1 Loss Collaborates with NRasG12D In Vivo

We and others previously reported that *ASXL1* mutations are most common in chronic myelomonocytic leukemia and frequently co-occur with *N/K-Ras* mutations in chronic

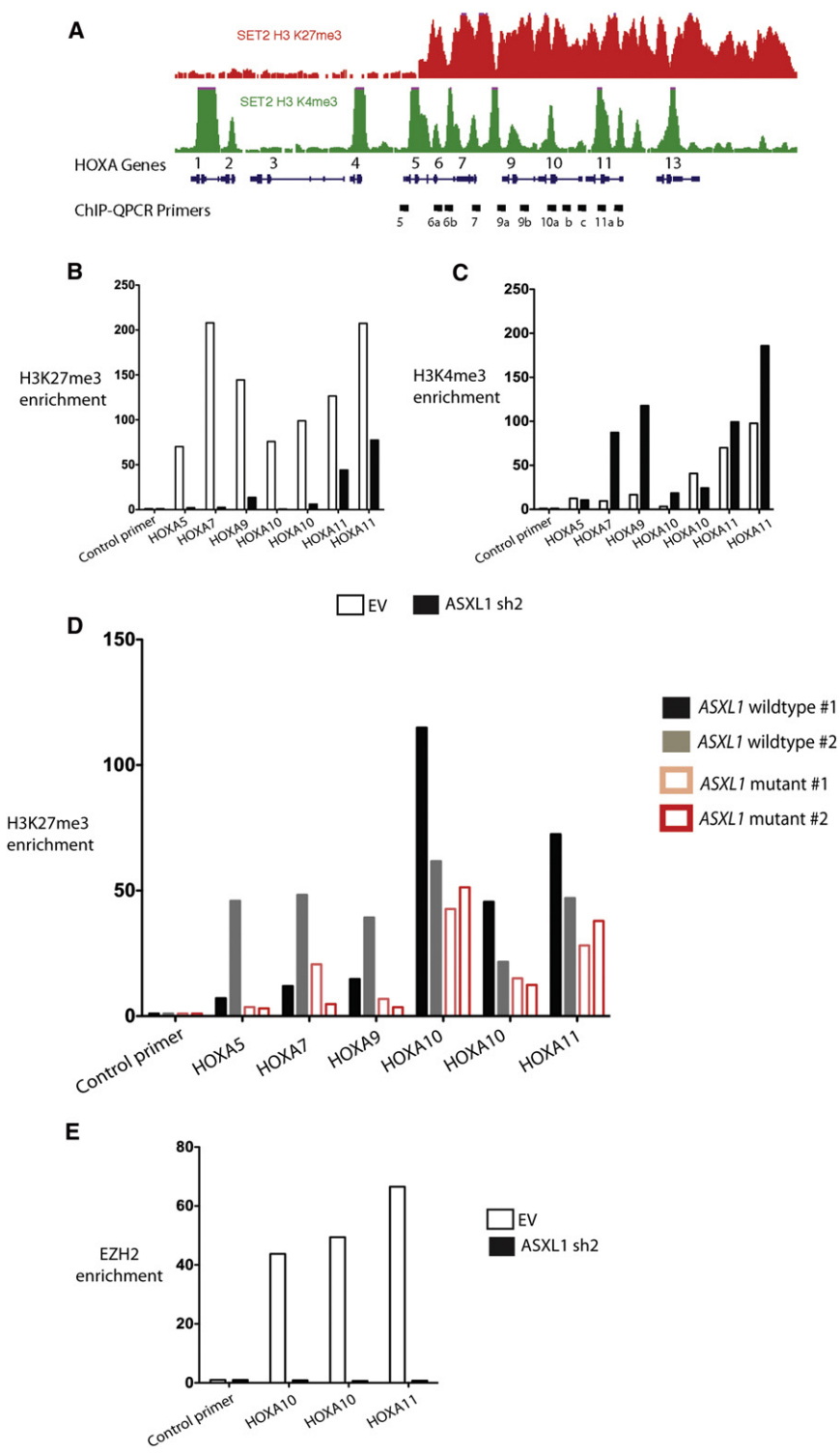


Figure 5. ASXL1 Loss Is Associated with Loss of PRC2 Recruitment at the HOXA Locus

(A) Chromatin-immunoprecipitation (ChIP) for H3K27me3 and H3K4me3 followed by next-generation sequencing reveals the abundance and localization of H3K27me3 and H3K4me3 at the *HoxA* locus in SET2 cells.

(B and C) ChIP for H3K27me3 (B) and H3K4me3 (C) followed by quantitative PCR (qPCR) across the 5' *HOXA* locus in SET2 cells treated with an empty vector or stable knockdown of ASXL1 reveals a consistent downregulation of H3K27me3 across the 5' *HOXA* locus following ASXL1 loss and a modest increase in H3K4me3 at the promoters of 5' *HOXA* genes with ASXL1 loss [primer locations are shown in (A)].

(D) Similar ChIP for H3K27me3 followed by qPCR across the *HOXA* locus in primary leukemic blasts from two patients with ASXL1 mutations versus two without ASXL1 mutations reveals H3K27me3 loss across the *HOXA* locus in ASXL1 mutant cells.

(E) ChIP for EZH2 followed by qPCR at the 5' end of *HOXA* locus in SET2 cells reveals loss of EZH2 enrichment with ASXL1 loss in SET2 cells. ChIP-qPCR was performed in biologic duplicates and ChIP-qPCR data is displayed as enrichment relative to input. qPCR at the gene body of *RRP1*, a region devoid of H3K4me3 or H3K27me3, is utilized as a control locus.

The error bars represent standard deviation.

cells into lethally irradiated recipient mice. We validated our ability to effectively knock down ASXL1 in vivo by performing qRT-PCR in hematopoietic cells from recipient mice (Figure 7A and Figure S6A). Consistent with our in vitro data implicating the *HoxA* cluster as an ASXL1 target locus, we noted a marked increase in *HoxA9* and *HoxA10* expression in bone marrow nucleated cells from mice expressing *NRasG12D* in combination with *Asxl1* shRNA compared to mice expressing *NRasG12D* alone (Figure 7B).

Expression of oncogenic *NRasG12D* and an empty shRNA vector control led to a progressive myeloproliferative disorder as previously described (Mackenzie et al., 1999). In contrast, expression of *NRasG12D* in combination with validated *mASXL1* knockdown vectors re-

myelomonocytic leukemia (Abdel-Wahab et al., 2011; Patel et al., 2010). We therefore investigated the effects of combined *NRasG12D* expression and *Asxl1* loss in vivo. To do this, we expressed *NRasG12D* in combination with an empty vector expressing GFP alone or one of two different *Asxl1* shRNA constructs in whole bone marrow cells and transplanted these

resulted in accelerated myeloproliferation and impaired survival compared with mice transplanted with *NRasG12D/EV* (median survival 0.8 month for ASXL1 shRNA versus 3 months for control shRNA vector: $p < 0.005$; Figure 7C) We also noted impaired survival with an independent *mASXL1* shRNA construct ($p < 0.01$; Figure S6B) Mice transplanted with *NRasG12D/Asxl1*

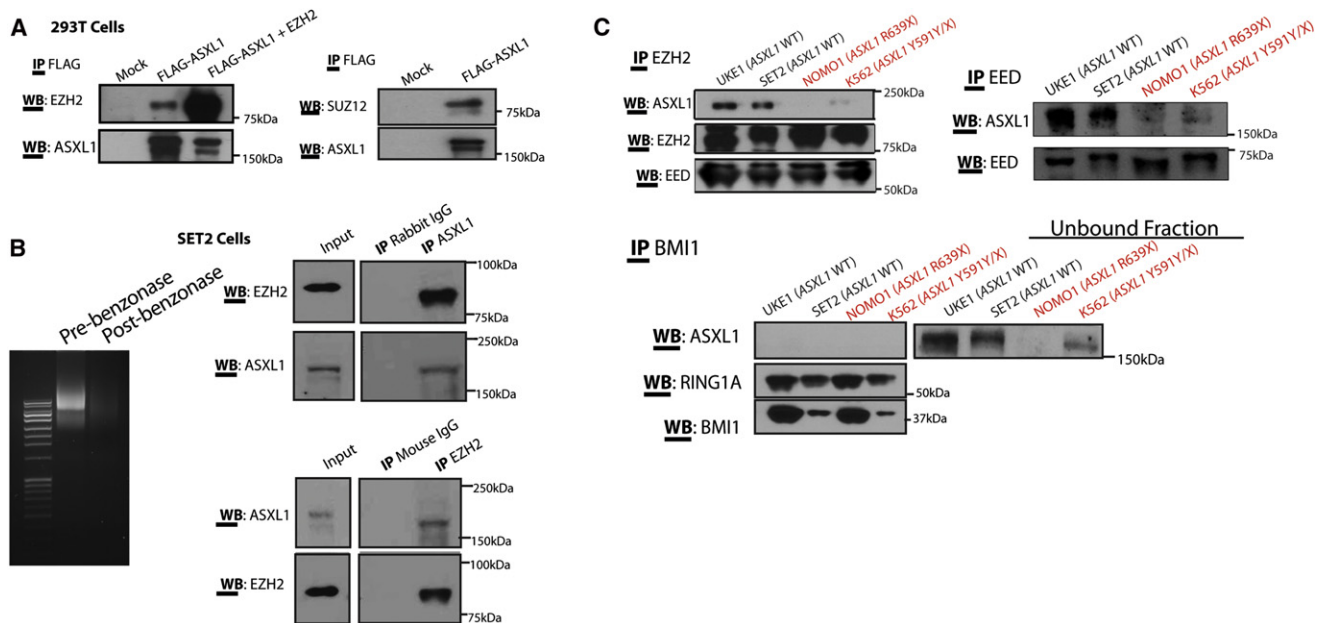


Figure 6. ASXL1 Interacts with the PRC2 in Hematopoietic Cells

(A) Physical interaction between ASXL1 and EZH2 is demonstrated by transient transfection of HEK293T cells with FLAG-hASXL1 cDNA with or without hEZH2 cDNA followed by immunoprecipitation (IP) of FLAG epitope and western blotting for EZH2 and ASXL1.

(B) HEK293T cells were transiently transfected with FLAG-hASXL1 cDNA followed by IP of FLAG epitope and western blotting for SUZ12 and ASXL1. Endogenous interaction of ASXL1 with PRC2 members was also demonstrated by IP of endogenous EZH2 and ASXL1 followed by western blotting of the other proteins in whole cell lysates from SET2 cells.

(C) Lysates from the experiment shown in (B) were treated with benzonase to ensure nucleic acid free conditions in the lysates prior to IP as shown by ethidium bromide staining of an agarose gel before and after benzonase treatment. IP of endogenous EZH2 and embryonic ectoderm development (EED) in a panel of ASXL1-wild-type and mutant human leukemia cells reveals a specific interaction between ASXL1 and PRC2 members in ASXL1-wildtype human myeloid leukemia cells. In contrast, IP of the PRC1 member BMI1 failed to pull down ASXL1.

See also Figure S5.

shRNA had increased splenomegaly and hepatomegaly compared with *NRasG12D/EV* transplanted mice (Figures 7D and 7E; Figure S6C). Histological analysis revealed a significant increase in myeloid infiltration of the spleen and livers of mice transplanted with *NRasG12D/Asx1* shRNA (Figure S6D).

Mice transplanted with *NRasG12D/Asx1* shRNA, but not *NRasG12D/EV*, experienced progressive, severe anemia (Figure 7F). It has previously been identified that expression of oncogenic *K/N-Ras* in multiple models of human/murine hematopoietic systems results in alterations in the erythroid compartment (Braun et al., 2006; Darley et al., 1997; Zhang et al., 2003). We noted an expansion of CD71^{high}/Ter119^{high} erythroblasts in the bone marrow of mice transplanted with *NRasG12D/Asx1* shRNA compared with *NRasG12D/EV* mice (Figure S6E). We also noted increased granulocytic expansion in mice engrafted with *NRasG12D/Asx1* shRNA positive cells, as shown by the presence of increased neutrophils in the peripheral blood (Figure S6D) and the expansion of Gr1/Mac1 double-positive cells in the bone marrow by flow cytometry (Figure S6F).

Previous studies have shown that hematopoietic cells from mice expressing oncogenic *Ras* alleles or other mutations that activate kinase signaling pathways do not exhibit increased self-renewal in colony replating assays (Braun et al., 2004; MacKenzie et al., 1999). This is in contrast to the immortalization of hematopoietic cells in vitro seen with expression of *MLL-AF9*

(Somerville and Cleary, 2006) or deletion of *Tet2* (Moran-Crusio et al., 2011). Bone marrow cells from mice with combined overexpression of *NRasG12D* plus *Asx1* knockdown had increased serial replating (to five passages) compared to bone marrow cells from mice engrafted with *NRasG12D/EV* cells (Figure 7G). These studies demonstrate that *Asx1* loss cooperates with oncogenic *NRasG12D* in vivo.

DISCUSSION

The data presented here identify that ASXL1 loss in hematopoietic cells results in reduced H3K27me3 occupancy through inhibition of PRC2 recruitment to specific oncogenic target loci. Recent studies have demonstrated that genetic alterations in the PRC2 complex occur in a spectrum of human malignancies (Bracken and Helin, 2009; Margueron and Reinberg, 2011; Sauvageau and Sauvageau, 2010). Activating mutations and overexpression of *EZH2* occur most commonly in epithelial malignancies and in lymphoid malignancies (Morin et al., 2010; Varambally et al., 2002). However, there are increasing genetic data implicating mutations that impair PRC2 function in the pathogenesis of myeloid malignancies. These include the loss-of-function mutations in *EZH2* (Abdel-Wahab et al., 2011; Ernst et al., 2010; Nikoloski et al., 2010) and less common somatic loss-of-function mutations in *SUZ12*, *EED*, and *JARID2* (Score

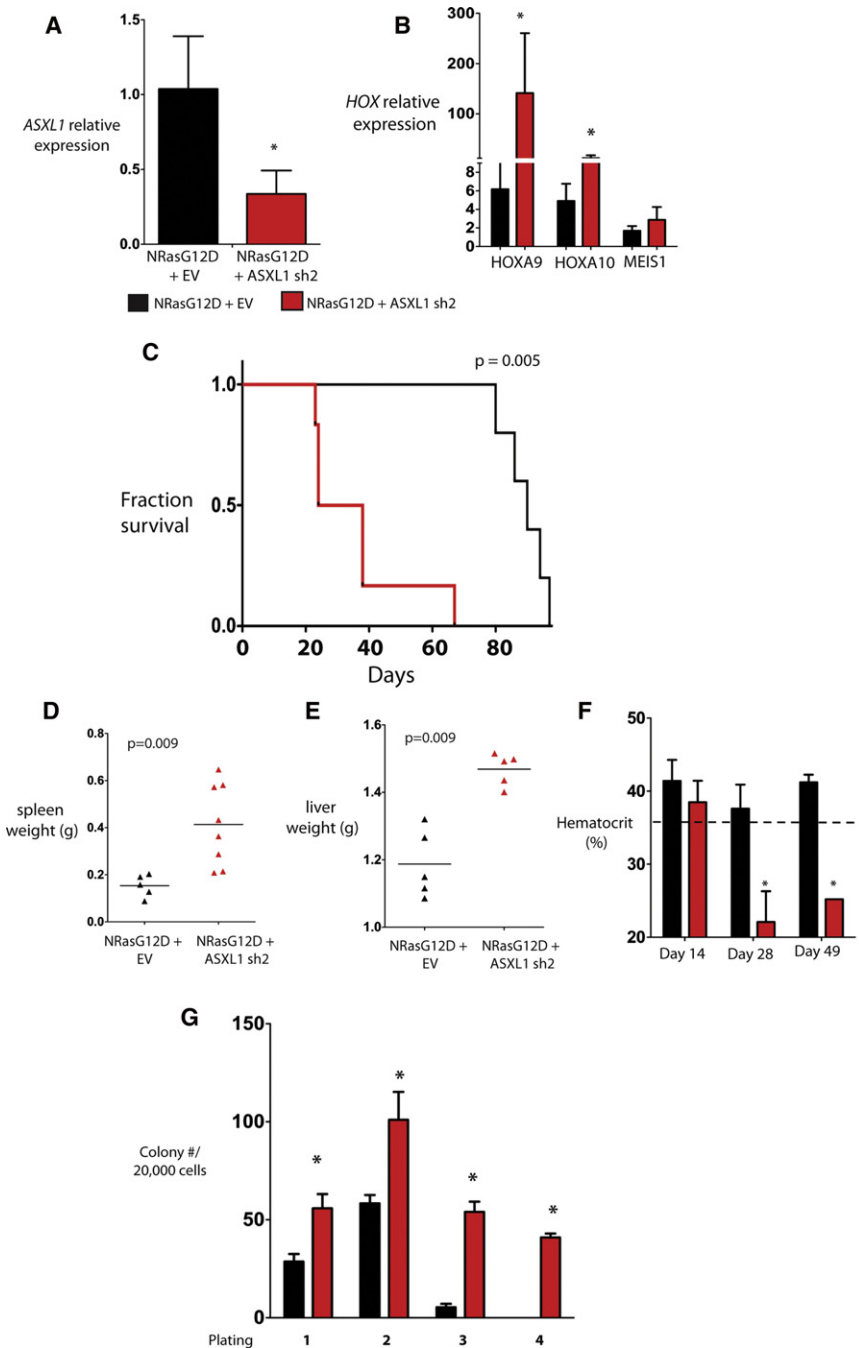


Figure 7. Asx1 Silencing Cooperates with NRasG12D In Vivo

(A) Retroviral bone marrow transplantation of NRasG12D with or without an shRNA for Asx1 resulted in decreased *Asx1* mRNA expression as shown by qRT-PCR results in nucleated peripheral blood cells from transplanted mice at 14 days following transplant.

(B) qRT-PCR revealed an increased expression of *HOXA9* and *HOXA10* but not *MEIS1* in the bone marrow of mice sacrificed 19 days following transplantation.

(C) Transplantation of bone marrow cells bearing overexpression of NRasG12D in combination with downregulation of *Asx1* led to a significant hastening of death compared to mice transplanted with NRasG12D/EV.

(D–F) Mice transplanted with NRasG12D/ASXL1 shRNA experienced increased splenomegaly (D) and hepatomegaly (E), and progressive anemia (F) compared with mice transplanted with NRasG12D + an empty vector (EV).

(G) Bone marrow cells from mice with combined NRasG12D overexpression/Asx1 knockdown revealed increased serial replating compared with cells from NRasG12D/EV mice. Error bars represent standard deviation relative to control. Asterisk indicates $p < 0.05$ (two-tailed, Mann Whitney U test).

See also Figure S6.

myeloid malignancies. In many cases, patients present with concomitant heterozygous mutations in multiple PRC2 members or in *EZH2* and *ASXL1*; these data suggest that haploinsufficiency for multiple genes that regulate PRC2 function can cooperate in hematopoietic transformation through additive alterations in PRC2 function.

Many studies have investigated how mammalian PcG proteins are recruited to chromatin in order to repress gene transcription and specify cell fate in different tissue contexts. Recent in silico analysis suggested that ASXL proteins found in animals contain a number of domains that likely serve in the recruitment of chromatin modulators and transcriptional effectors to DNA (Aravind and

et al., 2012) in patients with myeloproliferative neoplasms, myelodysplastic syndrome, and chronic myelomonocytic leukemia. The data from genetically-engineered mice also support this concept with *Ezh2* overexpression models, revealing evidence of promotion of malignant transformation (Herrera-Merchan et al., 2012), and recent studies demonstrate a role for *Ezh2* loss in leukemogenesis (Simon et al., 2012). Thus, it appears that alterations in normal PRC2 activity and/or H3K27me3 abundance in either direction may promote malignant transformation. Our data implicate *ASXL1* mutations as an additional genetic alteration that leads to impaired PRC2 function in patients with

Iyer, 2012). Data from ChIP and co-immunoprecipitation experiments presented here suggest a specific role for ASXL1 in epigenetic regulation of gene expression by facilitating PRC2-mediated transcriptional repression of known leukemic oncogenes. Thus, ASXL1 may serve as a scaffold for recruitment of the PRC2 complex to specific loci in hematopoietic cells, as has been demonstrated for JARID2 in embryonic stem cells (Landeira et al., 2010; Pasini et al., 2010; Peng et al., 2009; Shen et al., 2009).

Recent data suggested that ASXL1 might interact with BAP1 to form a H2AK119 deubiquitinase (Scheuermann et al., 2010).

However, our data suggest that ASXL1 loss leads to BAP1-independent alterations in chromatin state and gene expression in hematopoietic cells. These data are consonant with recent genetic studies, which have shown that germline loss of BAP1 increases susceptibility to uveal melanoma and mesothelioma (Testa et al., 2011; Wiesner et al., 2011). In contrast, germline loss of ASXL1 is seen in the developmental disorder Bohring-Opitz Syndrome (Hoischen et al., 2011), but has not, to date, been observed as a germline solid tumor susceptibility locus. Whether alterations in H2AK119 deubiquitinase function due to alterations in BAP1 and/or ASXL1 can contribute to leukemogenesis or to the pathogenesis of other malignancies remains to be determined.

Integration of gene expression and chromatin state data following ASXL1 loss identified specific loci with a known role in leukemogenesis that are altered in the setting of ASXL1 mutations. These include the posterior *HOXA* cluster, including *HOXA9*, which has a known role in hematopoietic transformation. We demonstrate that ASXL1 normally serves to tightly regulate *HOXA* gene expression in hematopoietic cells, and that loss of ASXL1 leads to disordered *HOXA* gene expression in vitro and in vivo. Overexpression of 5' *HOXA* genes is a well-described oncogenic event in hematopoietic malignancies (Lawrence et al., 1996), and previous studies have shown that *HOXA9* overexpression leads to transformation in vitro and in vivo when co-expressed with *MEIS1* (Kroon et al., 1998). Interestingly, ASXL1 loss was not associated with an increase in *MEIS1* expression, suggesting that transformation by ASXL1 mutations requires the co-occurrence of oncogenic disease alleles which dysregulate additional target loci. These data and our in vivo studies suggest that ASXL1 loss, in combination with co-occurring oncogenes, can lead to hematopoietic transformation and increased self-renewal. Further studies in mice expressing ASXL1 shRNA or with conditional deletion of *Asx1* alone and in concert with leukemogenic disease alleles will provide additional insight into the role of ASXL1 loss in hematopoietic stem/progenitor function and in leukemogenesis.

Given that somatic mutations in chromatin modifying enzymes (Dagliesh et al., 2010), DNA methyltransferases (Ley et al., 2010), and other genes implicated in epigenetic regulation occur commonly in human cancers, it will be important to use epigenomic platforms to elucidate how these disease alleles contribute to oncogenesis in different contexts. The data here demonstrate how integrated epigenetic and functional studies can be used to elucidate the function of somatic mutations in epigenetic modifiers. In addition, it is likely that many known oncogenes and tumor suppressors contribute, at least in part, to transformation through direct or indirect alterations in the epigenetic state (Dawson et al., 2009). Subsequent epigenomic studies of human malignancies will likely uncover novel routes to malignant transformation in different malignancies, and therapeutic strategies that reverse epigenetic alterations may be of specific benefit in patients with mutations in epigenetic modifiers.

EXPERIMENTAL PROCEDURES

Cell Culture

HEK293T cells were cultured in Dulbecco's modified Eagle's medium (DMEM) supplemented with 10% fetal bovine serum (FBS) and nonessential amino

acids. Human leukemia cell lines were cultured in RPMI-1640 medium supplemented with 10% FBS+1 mM hydrocortisone+10% horse serum (UKE1 cells), RPMI-1640 supplemented with 10% FBS (K562, MOLM13, KCL22, KU812 cells), RPMI-1640 supplemented with 20% FBS (SET2, NOMO1, Monomac-6 cells), or IMDM + 20% FBS (KBM5 cells). For proliferation studies, 1×10^3 cells were seeded in 1 ml volume of media in triplicate and cell number was counted manually daily for 7 days by Trypan blue exclusion.

Plasmid Constructs, Mutagenesis Protocol, Short Hairpin RNA, and Small Interfering RNA

See Supplemental Information.

Primary Acute Myeloid Leukemia Patient Samples and ASXL1, BAP1, EZH2, SUZ12, and EED Genomic DNA Sequencing Analysis

Approval was obtained from the institutional review boards at Memorial Sloan-Kettering Cancer Center and at the Hospital of the University of Pennsylvania for these studies, and informed consent was provided according to the Declaration of Helsinki. Please see Supplemental Information for details on DNA sequence analysis.

Western Blot and Immunoprecipitation Analysis

Western blots were carried out using the following antibodies: ASXL1 (Clone N-13; Santa Cruz (sc-85283); N-terminus directed), ASXL1 (Clone 2049C2a; Santa Cruz (sc-81053); C terminus directed), BAP1 [clone 3C11; Santa Cruz (sc-13576)], BMI1 (Abcam ab14389), EED (Abcam ab4469), EZH2 (Active Motif 39933 or Millipore 07-689), FLAG (M2 FLAG; Sigma A2220), Histone H3 lysine 27 trimethyl (Abcam ab6002), Histone H2A Antibody II (Cell Signaling Technologies 2578), Ubiquityl-Histone H2AK119 (Clone D27C4; Cell Signaling Technologies 8240), RING1A (Abcam ab32807), SUZ12 (Abcam ab12073), and total histone H3 (Abcam ab1791), and tubulin (Sigma, T9026). Antibodies different from the above used for immunoprecipitation include: ASXL1 [clone H105X; Santa Cruz (sc-98302)], FLAG (Novus Biological Products; NBP1-06712), and EZH2 (Active Motif 39901). Immunoprecipitation and pull-down reactions were performed in an immunoprecipitation buffer (150 mM NaCl, 20 mM Tris (pH 7.4–7.5), 5 mM EDTA, 1% Triton, 100 mM sodium orthovanadate, protease arrest (Genotec), 1 mM PMSF, and phenylarsene oxide). To ensure nuclease-free immunoprecipitation conditions, immunoprecipitations were also performed using the following methodology (Muntean et al., 2010): cells were lysed in BC-300 buffer (20 mM Tris-HCl (pH 7.4), 10% glycerol, 300 mM KCl, 0.1% NP-40) and the cleared lysate was separated from the insoluble pellet and treated with MgCl₂ to 2.5 mM and benzonase (Emanuel Merck, Darmstadt) at a concentration of 1,250 U/ml. The lysate was then incubated for 1–1.5 hr at 4°. The reaction was then stopped with addition of 5 mM EDTA. DNA digestion is confirmed on an ethidium bromide agarose gel. We then set up our immunoprecipitation by incubating our lysate overnight at 4°.

Histone Extraction and Histone LC/MS Analysis

See Supplemental Information.

Gene Expression Analysis

Total RNA was extracted from cells using QIAGEN's RNeasy Plus Mini kit (Valencia, CA, USA). cDNA synthesis, labeling, hybridization, and quality control were carried out as previously described (Figuroa et al., 2008). Ten micrograms of RNA was then used for generation of labeled cRNA according to the manufacturer's instructions (Affymetrix, Santa Clara, CA, USA). Hybridization of the labeled cRNA fragments and washing, staining, and scanning of the arrays were carried out as per instructions of the manufacturer. Labeled cRNA from CD34+ cells treated with either ASXL1 siRNA or controls were analyzed using the Affymetrix HG-U133-Plus2.0 platform and from UKE1 cells using the Illumina Href8 array. All expression profile experiments were carried out using biological duplicates. "Present" calls in $\geq 80\%$ of samples were captured and quantile normalized across all samples on a per-chip basis. Raw expression values generated by Genome Studio (Illumina) were filtered to exclude probesets having expression values below negative background in $\geq 80\%$ of samples. Probesets remaining after background filtering were log₂ transformed and quantile normalized on a per-chip basis. qRT-PCR was performed on cDNA using SYBR green quantification in an ABI 7500

sequence detection system. The sequences of all qRT-PCR primers are listed in the Supplemental Information.

Chromatin Immunoprecipitation and Antibodies

ChIP experiments for H3K4me3, H3K27me3, and H3K36me3 were carried out as described previously (Bernstein et al., 2006; Mikkelsen et al., 2007). Cells were cross-linked in 1% formaldehyde, lysed, and sonicated with a Branson 250 Sonifier to obtain chromatin fragments in a size range between 200 and 700 bp. Solubilized chromatin was diluted in ChIP dilution buffer (1:10) and incubated with antibody overnight at 4°C. Protein A sepharose beads (Sigma) were used to capture the antibody-chromatin complex and washed with low salt, LiCl, as well as TE (pH 8.0) wash buffers. Enriched chromatin fragments were eluted at 65°C for 10 min, subjected to cross-link reversal at 65°C for 5 hr, and treated with Proteinase K (1 mg/ml), before being extracted by phenol-chloroform-isoamyl alcohol, and ethanol precipitated. ChIP DNA was then quantified by QuantiT Picogreen dsDNA Assay kit (Invitrogen). ChIP experiments for ASXL1 were carried out on nuclear preps. Cross-linked cells were incubated in swelling buffer (0.1 M Tris pH 7.6, 10 mM KOAc, 15 mM MgOAc, 1% NP40), on ice for 20 minutes, passed through a 16G needle 20 times and centrifuged to collect nuclei. Isolated nuclei were then lysed, sonicated, and immunoprecipitated as described above. Antibodies used for ChIP include anti-H3K4me3 (Abcam ab8580), anti-H3K27me3 (Upstate 07-449), anti-H3K36me3 (Abcam ab9050), and anti-ASXL1 [clone H105X; Santa Cruz (sc-98302)], and Ubiquitinyl-Histone H2AK119 (Clone D27C4; Cell Signaling Technologies 8240).

Sequencing Library Preparation, Illumina/Solexa Sequencing, and Read Alignment and Generation of Density Maps

See Supplemental Information.

HOXA Nanostring nCounter Gene Expression CodeSet

Direct digital mRNA analysis of *HOXA* cluster gene expression was performed using a Custom CodeSet including each *HOXA* gene (NanoString Technologies). Synthesis of the oligonucleotides was done by NanoString Technologies, and hybridization and analysis were done using the Prep Station and Digital Analyzer purchased from the company.

Animal Use, Retroviral Bone Marrow Transplantation, Flow Cytometry, and Colony Assays

Animal care was in strict compliance with institutional guidelines established by the Memorial Sloan-Kettering Cancer Center, the National Academy of Sciences Guide for the Care and Use of Laboratory Animals, and the Association for Assessment and Accreditation of Laboratory Animal Care International. All animal procedures were approved by the Institutional Animal Care and Use Committee (IACUC) at Memorial Sloan-Kettering Cancer Center. See Supplemental Information for more details on animal experiments.

Statistical Analysis

Statistical significance was determined by the Mann-Whitney U test and Fisher's exact test using Prism GraphPad software. Significance of survival differences was calculated using Log-rank (Mantel-Cox) test. $p < 0.05$ was considered statistically significant. Normalized expression data from CD34+ cord blood was used as a Gene Set Enrichment Analysis query of the C2 database (MSig DB) where 1,000 permutations of the genes was used to generate a null distribution. A pre-ranked gene list, containing genes upregulated at least \log_2 0.5-fold, in which the highest ranked genes corresponds to the genes, with the largest fold-difference between *Asxl1* hairpin-treated UKE1 cells and those treated with empty vector, was used to query the C2 MSig DB as described above.

ACCESSION NUMBERS

All microarray data used in this manuscript are deposited in Gene Expression Omnibus (<http://www.ncbi.nlm.nih.gov/geo/>) under GEO accession number GSE38692. The ChIP-Seq data are deposited under GEO accession number GSE38861.

SUPPLEMENTAL INFORMATION

Supplemental Information includes six figures, two tables, and Supplemental Experimental Procedures and can be found with this article online at <http://dx.doi.org/10.1016/j.ccr.2012.06.032>.

ACKNOWLEDGMENTS

This work was supported by a grant from the Starr Cancer Consortium to R.L.L. and B.E.B., by grants from the Gabrielle's Angel Fund to R.L.L. and O.A.-W., by a grant from the Anna Fuller Fund to R.L.L., and by an NHLBI grant to B.E.B. (5U01HL100395). I.A. and B.E.B. are Howard Hughes Medical Institute Early Career Scientists. A.M. is a Burroughs Wellcome Clinical Translational Scholar and Scholar of the Leukemia and Lymphoma Society. X.Z. and S.D.N. are supported by a Leukemia and Lymphoma Society SCOR award, and F.P. is supported by an American Italian Cancer Foundation award. O.A.-W. is an American Society of Hematology Basic Research Fellow and is supported by a grant from the NIH K08 Clinical Investigator Award (1K08CA160647-01). J.P.P. is supported by an American Society of Hematology Trainee Research Award.

Received: January 7, 2012

Revised: May 21, 2012

Accepted: June 28, 2012

Published: August 13, 2012

REFERENCES

- Abdel-Wahab, O., Pardanani, A., Patel, J., Wadleigh, M., Lasho, T., Heguy, A., Beran, M., Gilliland, D.G., Levine, R.L., and Tefferi, A. (2011). Concomitant analysis of EZH2 and ASXL1 mutations in myelofibrosis, chronic myelomonocytic leukemia and blast-phase myeloproliferative neoplasms. *Leukemia* 25, 1200–1202.
- Aravind, L., and Iyer, L.M. (2012). The HARE-HTH and associated domains: Novel modules in the coordination of epigenetic DNA and protein modifications. *Cell Cycle* 11, 119–131.
- Bejar, R., Stevenson, K., Abdel-Wahab, O., Galili, N., Nilsson, B., Garcia-Manero, G., Kantarjian, H., Raza, A., Levine, R.L., Neuberg, D., and Ebert, B.L. (2011). Clinical effect of point mutations in myelodysplastic syndromes. *N. Engl. J. Med.* 364, 2496–2506.
- Bernstein, B.E., Mikkelsen, T.S., Xie, X., Kamal, M., Huebert, D.J., Cuff, J., Fry, B., Meissner, A., Wernig, M., Plath, K., et al. (2006). A bivalent chromatin structure marks key developmental genes in embryonic stem cells. *Cell* 125, 315–326.
- Bott, M., Brevet, M., Taylor, B.S., Shimizu, S., Ito, T., Wang, L., Creaney, J., Lake, R.A., Zakowski, M.F., Reva, B., et al. (2011). The nuclear deubiquitinase BAP1 is commonly inactivated by somatic mutations and 3p21.1 losses in malignant pleural mesothelioma. *Nat. Genet.* 43, 668–672.
- Bracken, A.P., and Helin, K. (2009). Polycomb group proteins: navigators of lineage pathways led astray in cancer. *Nat. Rev. Cancer* 9, 773–784.
- Braun, B.S., Tuveson, D.A., Kong, N., Le, D.T., Kogan, S.C., Rozmus, J., Le Beau, M.M., Jacks, T.E., and Shannon, K.M. (2004). Somatic activation of oncogenic *Kras* in hematopoietic cells initiates a rapidly fatal myeloproliferative disorder. *Proc. Natl. Acad. Sci. USA* 101, 597–602.
- Braun, B.S., Archard, J.A., Van Ziffle, J.A., Tuveson, D.A., Jacks, T.E., and Shannon, K. (2006). Somatic activation of a conditional *KrasG12D* allele causes ineffective erythropoiesis in vivo. *Blood* 108, 2041–2044.
- Cho, Y.S., Kim, E.J., Park, U.H., Sin, H.S., and Um, S.J. (2006). Additional sex comb-like 1 (ASXL1), in cooperation with SRC-1, acts as a ligand-dependent coactivator for retinoic acid receptor. *J. Biol. Chem.* 281, 17588–17598.
- Dalgliesh, G.L., Furge, K., Greenman, C., Chen, L., Bignell, G., Butler, A., Davies, H., Edkins, S., Hardy, C., Latimer, C., et al. (2010). Systematic sequencing of renal carcinoma reveals inactivation of histone modifying genes. *Nature* 463, 360–363.

- Dantuma, N.P., Groothuis, T.A., Salomons, F.A., and Neeffjes, J. (2006). A dynamic ubiquitin equilibrium couples proteasomal activity to chromatin remodeling. *J. Cell Biol.* *173*, 19–26.
- Darley, R.L., Hoy, T.G., Baines, P., Padua, R.A., and Burnett, A.K. (1997). Mutant N-RAS induces erythroid lineage dysplasia in human CD34+ cells. *J. Exp. Med.* *185*, 1337–1347.
- Dawson, M.A., Bannister, A.J., Göttgens, B., Foster, S.D., Bartke, T., Green, A.R., and Kouzarides, T. (2009). JAK2 phosphorylates histone H3Y41 and excludes HP1alpha from chromatin. *Nature* *461*, 819–822.
- Ernst, T., Chase, A.J., Score, J., Hidalgo-Curtis, C.E., Bryant, C., Jones, A.V., Waghorn, K., Zoi, K., Ross, F.M., Reiter, A., et al. (2010). Inactivating mutations of the histone methyltransferase gene EZH2 in myeloid disorders. *Nat. Genet.* *42*, 722–726.
- Figuerola, M.E., Reimers, M., Thompson, R.F., Ye, K., Li, Y., Selzer, R.R., Fridriksson, J., Paietta, E., Wiernik, P., Green, R.D., et al. (2008). An integrative genomic and epigenomic approach for the study of transcriptional regulation. *PLoS One* *3*, e1882.
- Fisher, C.L., Lee, I., Bloyer, S., Bozza, S., Chevalier, J., Dahl, A., Bodner, C., Helgason, C.D., Hess, J.L., Humphries, R.K., and Brock, H.W. (2010a). Additional sex combs-like 1 belongs to the enhancer of trithorax and polycomb group and genetically interacts with Cbx2 in mice. *Dev. Biol.* *337*, 9–15.
- Fisher, C.L., Pineault, N., Brookes, C., Helgason, C.D., Ohta, H., Bodner, C., Hess, J.L., Humphries, R.K., and Brock, H.W. (2010b). Loss-of-function Additional sex combs-like1 mutations disrupt hematopoiesis but do not cause severe myelodysplasia or leukemia. *Blood* *115*, 38–46.
- Gaebler, C., Stanzl-Tschegg, S., Heinze, G., Holper, B., Milne, T., Berger, G., and Vécsei, V. (1999). Fatigue strength of locking screws and prototypes used in small-diameter tibial nails: a biomechanical study. *J. Trauma* *47*, 379–384.
- Gelsi-Boyer, V., Trouplin, V., Adélaïde, J., Bonansea, J., Cervera, N., Carbuccia, N., Lagarde, A., Prebet, T., Nezri, M., Sainty, D., et al. (2009). Mutations of polycomb-associated gene ASXL1 in myelodysplastic syndromes and chronic myelomonocytic leukaemia. *Br. J. Haematol.* *145*, 788–800.
- Harbour, J.W., Onken, M.D., Roberson, E.D., Duan, S., Cao, L., Worley, L.A., Council, M.L., Matatall, K.A., Helms, C., and Bowcock, A.M. (2010). Frequent mutation of BAP1 in metastasizing uveal melanomas. *Science* *330*, 1410–1413.
- Herrera-Merchan, A., Arranz, L., Ligos, J.M., de Molina, A., Dominguez, O., and Gonzalez, S. (2012). Ectopic expression of the histone methyltransferase Ezh2 in haematopoietic stem cells causes myeloproliferative disease. *Nat Commun* *3*, 623.
- Hoischen, A., van Bon, B.W., Rodríguez-Santiago, B., Gilissen, C., Vissers, L.E., de Vries, P., Janssen, I., van Lier, B., Hastings, R., Smithson, S.F., et al. (2011). De novo nonsense mutations in ASXL1 cause Bohring-Opitz syndrome. *Nat. Genet.* *43*, 729–731.
- Kroon, E., Kros, J., Thorsteinsdottir, U., Baban, S., Buchberg, A.M., and Sauvageau, G. (1998). Hoxa9 transforms primary bone marrow cells through specific collaboration with Meis1a but not Pbx1b. *EMBO J.* *17*, 3714–3725.
- Kumar, A.R., Li, Q., Hudson, W.A., Chen, W., Sam, T., Yao, Q., Lund, E.A., Wu, B., Kowal, B.J., and Kersey, J.H. (2009). A role for MEIS1 in MLL-fusion gene leukemia. *Blood* *113*, 1756–1758.
- Landeira, D., Sauer, S., Poot, R., Dvorkina, M., Mazzarella, L., Jorgensen, H.F., Pereira, C.F., Leleu, M., Piccolo, F.M., Spivakov, M., et al. (2010). Jarid2 is a PRC2 component in embryonic stem cells required for multi-lineage differentiation and recruitment of PRC1 and RNA Polymerase II to developmental regulators. *Nat. Cell Biol.* *12*, 618–624.
- Lawrence, H.J., Sauvageau, G., Humphries, R.K., and Largman, C. (1996). The role of HOX homeobox genes in normal and leukemic hematopoiesis. *Stem Cells* *14*, 281–291.
- Lee, S.W., Cho, Y.S., Na, J.M., Park, U.H., Kang, M., Kim, E.J., and Um, S.J. (2010). ASXL1 represses retinoic acid receptor-mediated transcription through associating with HP1 and LSD1. *J. Biol. Chem.* *285*, 18–29.
- Ley, T.J., Ding, L., Walter, M.J., McLellan, M.D., Lamprecht, T., Larson, D.E., Kandath, C., Payton, J.E., Baty, J., Welch, J., et al. (2010). DNMT3A mutations in acute myeloid leukemia. *N. Engl. J. Med.* *363*, 2424–2433.
- MacKenzie, K.L., Dolnikov, A., Millington, M., Shounan, Y., and Symonds, G. (1999). Mutant N-ras induces myeloproliferative disorders and apoptosis in bone marrow repopulated mice. *Blood* *93*, 2043–2056.
- Margueron, R., and Reinberg, D. (2011). The Polycomb complex PRC2 and its mark in life. *Nature* *469*, 343–349.
- Metzeler, K.H., Becker, H., Maharry, K., Radmacher, M.D., Kohlschmidt, J., Mrózek, K., Nicolet, D., Whitman, S.P., Wu, Y.Z., Schwind, S., et al. (2011). ASXL1 mutations identify a high-risk subgroup of older patients with primary cytogenetically normal AML within the ELN Favorable genetic category. *Blood* *118*, 6920–6929.
- Mikkelsen, T.S., Ku, M., Jaffe, D.B., Issac, B., Lieberman, E., Giannoukos, G., Alvarez, P., Brockman, W., Kim, T.K., Koche, R.P., et al. (2007). Genome-wide maps of chromatin state in pluripotent and lineage-committed cells. *Nature* *448*, 553–560.
- Moran-Crusio, K., Reavie, L., Shih, A., Abdel-Wahab, O., Ndiaye-Lobry, D., Lobry, C., Figuerola, M.E., Vasanthakumar, A., Patel, J., Zhao, X., et al. (2011). Tet2 loss leads to increased hematopoietic stem cell self-renewal and myeloid transformation. *Cancer Cell* *20*, 11–24.
- Morin, R.D., Johnson, N.A., Severson, T.M., Mungall, A.J., An, J., Goya, R., Paul, J.E., Boyle, M., Woolcock, B.W., Kuchenbauer, F., et al. (2010). Somatic mutations altering EZH2 (Tyr641) in follicular and diffuse large B-cell lymphomas of germinal-center origin. *Nat. Genet.* *42*, 181–185.
- Muntean, A.G., Tan, J., Sitwala, K., Huang, Y., Bronstein, J., Connelly, J.A., Basur, V., Elenitoba-Johnson, K.S., and Hess, J.L. (2010). The PAF complex synergizes with MLL fusion proteins at HOX loci to promote leukemogenesis. *Cancer Cell* *17*, 609–621.
- Nikoloski, G., Langemeijer, S.M., Kuiper, R.P., Knops, R., Massop, M., Tönnissen, E.R., van der Heijden, A., Scheele, T.N., Vandenberghe, P., de Witte, T., et al. (2010). Somatic mutations of the histone methyltransferase gene EZH2 in myelodysplastic syndromes. *Nat. Genet.* *42*, 665–667.
- Park, U.H., Yoon, S.K., Park, T., Kim, E.J., and Um, S.J. (2011). Additional sex comb-like (ASXL) proteins 1 and 2 play opposite roles in adipogenesis via reciprocal regulation of peroxisome proliferator-activated receptor gamma. *J. Biol. Chem.* *286*, 1354–1363.
- Pasini, D., Cloos, P.A., Walfridsson, J., Olsson, L., Bukowski, J.P., Johansen, J.V., Bak, M., Tommerup, N., Rappilber, J., and Helin, K. (2010). JARID2 regulates binding of the Polycomb repressive complex 2 to target genes in ES cells. *Nature* *464*, 306–310.
- Peng, J.C., Valouev, A., Swigut, T., Zhang, J., Zhao, Y., Sidow, A., and Wysocka, J. (2009). Jarid2/Jumonji coordinates control of PRC2 enzymatic activity and target gene occupancy in pluripotent cells. *Cell* *139*, 1290–1302.
- Pratcorona, M., Abbas, S., Sanders, M., Koenders, J., Kavelaars, F., Erpelinck-Verschueren, C., Zeilemaker, A., Lowenberg, B., and Valk, P. (2012). Acquired mutations in ASXL1 in acute myeloid leukemia: prevalence and prognostic value. *Haematologica* *97*, 388–392.
- Sauvageau, M., and Sauvageau, G. (2010). Polycomb group proteins: multifaceted regulators of somatic stem cells and cancer. *Cell Stem Cell* *7*, 299–313.
- Scheuermann, J.C., de Ayala Alonso, A.G., Oktaba, K., Ly-Hartig, N., McGinty, R.K., Fraterman, S., Wilm, M., Muir, T.W., and Müller, J. (2010). Histone H2A deubiquitinase activity of the Polycomb repressive complex PR-DUB. *Nature* *465*, 243–247.
- Score, J., Hidalgo-Curtis, C., Jones, A.V., Winkelmann, N., Skinner, A., Ward, D., Zoi, K., Ernst, T., Stegelmann, F., Dohner, K., et al. (2012). Inactivation of polycomb repressive complex 2 components in myeloproliferative and myelodysplastic/myeloproliferative neoplasms. *Blood* *119*, 1208–1213.
- Shen, X., Kim, W., Fujiwara, Y., Simon, M.D., Liu, Y., Mysliwiec, M.R., Yuan, G.C., Lee, Y., and Orkin, S.H. (2009). Jumonji modulates polycomb activity and self-renewal versus differentiation of stem cells. *Cell* *139*, 1303–1314.
- Simon, C., Chagraoui, J., Kros, J., Gendron, P., Wilhelm, B., Lemieux, S., Boucher, G., Chagnon, P., Drouin, S., Lambert, R., et al. (2012). A key role

for EZH2 and associated genes in mouse and human adult T-cell acute leukemia. *Genes Dev.* 26, 651–656.

Sinclair, D.A., Milne, T.A., Hodgson, J.W., Shellard, J., Salinas, C.A., Kyba, M., Randazzo, F., and Brock, H.W. (1998). The Additional sex combs gene of *Drosophila* encodes a chromatin protein that binds to shared and unique Polycomb group sites on polytene chromosomes. *Development* 125, 1207–1216.

Somervaille, T.C., and Cleary, M.L. (2006). Identification and characterization of leukemia stem cells in murine MLL-AF9 acute myeloid leukemia. *Cancer Cell* 10, 257–268.

Takeda, A., Goolsby, C., and Yaseen, N.R. (2006). NUP98-HOXA9 induces long-term proliferation and blocks differentiation of primary human CD34+ hematopoietic cells. *Cancer Res.* 66, 6628–6637.

Testa, J.R., Cheung, M., Pei, J., Below, J.E., Tan, Y., Sementino, E., Cox, N.J., Dogan, A.U., Pass, H.I., Trusa, S., et al. (2011). Germline BAP1 mutations predispose to malignant mesothelioma. *Nat. Genet.* 43, 1022–1025.

Thol, F., Friesen, I., Damm, F., Yun, H., Weissinger, E.M., Krauter, J., Wagner, K., Chaturvedi, A., Sharma, A., Wichmann, M., et al. (2011). Prognostic significance of ASXL1 mutations in patients with myelodysplastic syndromes. *J. Clin. Oncol.* 29, 2499–2506.

Varambally, S., Dhanasekaran, S.M., Zhou, M., Barrette, T.R., Kumar-Sinha, C., Sanda, M.G., Ghosh, D., Pienta, K.J., Sewalt, R.G., Otte, A.P., et al. (2002). The polycomb group protein EZH2 is involved in progression of prostate cancer. *Nature* 419, 624–629.

Wiesner, T., Obenauf, A.C., Murali, R., Fried, I., Griewank, K.G., Ulz, P., Windpassinger, C., Wackernagel, W., Loy, S., Wolf, I., et al. (2011). Germline mutations in BAP1 predispose to melanocytic tumors. *Nat. Genet.* 43, 1018–1021.

Zhang, J., Socolovsky, M., Gross, A.W., and Lodish, H.F. (2003). Role of Ras signaling in erythroid differentiation of mouse fetal liver cells: functional analysis by a flow cytometry-based novel culture system. *Blood* 102, 3938–3946.